KERNFORSCHUNGSZENTRUM

KARLSRUHE

Februar 1974

KFK 1944
EUR 4973e

Institut für Angewandte Systemtechnik und Reaktorphysik
Projekt Schneller Brüter

Current Status of Knowledge of Molten Fuel/Sodium Thermal Interactions

L. Caldarola

GESELLSCHAFT
FÜR
KERNFORSCHUNG M.B.H.

KARLSRUHE

GESELLSCHAFT FÜR KERNFORSCHUNG M. B. H.
KARLSRUHE

KERNFORSCHUNGSZENTRUM KARLSRUHE

Februar 1974

KFK 1944
EUR 4973e

Institut für Angewandte Systemtechnik
und Reaktorphysik

Projekt Schneller Brüter

Current Status of Knowledge of Molten Fuel/ Sodium Thermal Interactions

by L. Caldarola (1)

Paper presented at the meeting of the european "Safety Working Group" (Coordinating Committee for Fast Reactors) held in Brussels on 26/27th February 1974

(1)
Euratom delegate to the Karlsruhe fast reactor project

Current Status of Knowledge of Molten Fuel/ Sodium Thermal Interactions

by

L. Caldarola

Abstract

The papers which were presented at the CREST second specialist meeting on "Sodium/Fuel Interaction in Fast Reactors", held in Ispra in November 1973 are briefly reviewed. Some interesting conclusions are obtained based on the experimental and theoretical results presented at the meeting. Finally the areas for further investigations are specified.

Wissensstand über die thermische Wechselwirkung zwischen geschmolzenem Brennstoff und Natrium

von

L. Caldarola

Kurzfassung

Es wird ein kurzer Überblick gegeben über die Vorträge, die auf der 2. CREST-Fachtagung über "Sodium/Fuel Interaction in Fast Reactors" in Ispra im November 1973 gehalten wurden. Ausgehend von den auf der Tagung genannten experimentellen und theoretischen Ergebnissen, werden einige interessante Schlußfolgerungen gezogen. Schließlich werden weitere Bereiche für Untersuchungen angegeben.

Contents

1. Introduction

"Fuel-coolant interactions in a LMFBR become of interest in accident sequences when a substantial amount of fuel becomes molten and can come into contact with sodium. The interaction between molten fuel and coolant does not occur in a single distinct manner that can be described by one unique pressure-time history or by one unique thermal-to-mechanical energy-conversion ratio. Instead there are a number of different types of potential interactions between molten fuel and coolant." (Ref. 5).

Fuel-coolant interactions are of importance in two ways. First, they are of importance in characterizing fuel and coolant motion in an initiating accident where fuel pins fail. Secondly, they are of major importance in characterizing the damage potential from whole-core accidents if disassembly results. Experimental research programs have been started in various countries with the purpose of investigating fuel coolant interaction (FCI) in order to understand its mechanism, to measure its violence, as well as to evaluate consequences on the surrounding structures. Here we shall deal mainly with the first two aspects, which were the main topics at the CREST specialist meeting organized by the OECD and held at Ispra from the 21st to the 23rd November 1973. Experiments have been carried out in which various realistic reactor conditions were simulated. However, due to the multiplicity of the phenomena which occur, the interpretation of these experiments is very difficult. For this reason other experiments have been carried out which should ease theoretical interpretation. These experiments may be performed under unrealistic conditions (which do not occur in a LMFBR) and/or with different materials. In general the experiments can be classified in three large cathegories:

1. In-pile Tests. These tests are carried out in special test reactors (TREAT, RCN test reactor, CABRI etc) where various reactor accidents are simulated (overpower transients, loss of coolant accidents etc). Material composition and geometry are always carefully simulated.
2. Out of pile Tests. These tests are carried out in sodium but not in a test reactor. The condition under which UO_2 and Na come into contact are sometime unrealistic, with respect to reactor conditions.
3. Simulation Experiments
   These tests are conducted always in transparent liquids (water in most cases). This allows one to photograph the interaction zone by means of

high speed cameras and therefore, to gain a better insight into the physical phenomena which occur during the interaction. In general these experiments are carried out under unrealistic conditions, which do not occur in a LMFBR.

In parallel to these experimental programs, a second approach is being followed, namely, that of assuming that a large FCI can occur and of evaluating its consequences. New theoretical parametric models have been developed with the scope of analysing FCI in order to reduce the degree of conservatism which was imposed by early methods.
The objectives of this report are the following

1. To review the papers which were presented at the already mentioned OECD meeting at Ispra in order to give a synthetic picture of the present situation of the various experimental programs as well as of the parametric models (sections 2 and 3).
2. To discuss the results already obtained and to draw some conclusions (section 4).
3. To indicate areas in which further investigation is needed (section 5).

2. Review of the experimental programs and results reported in the papers presented at the Ispra conference

2.1 In pile Tests

2.1.1 TREAT-Tests (ANL-USA) (Ref. 5)

Three different types of tests were conducted at TREAT.

S-Tests. These tests were performed to investigate the transient pressure generated and the mechanical work done by the meltdown of clad fuel pins in sodium under conditions of very energetic overpower transients (2000-7000 Joule/gr of UO_2). Twelve tests have been carried out in stagnant sodium at an initial temperature ranging from 150°C to 500°C with masses of UO_2 ranging from 28 gr (1 pin) to 286 (7 pins). In general, several pressure pulses occured in each test. Peak pressures were measured from 40 to 150 atm. The energy conversion ratio was very low (from 8.10^{-6} to 10^{-3}). The most important result of these tests is that there were no energetic coherent interactions of the molten fuel and coolant. It appears likely that the initial pressure pulses and mechanical work measured can be explained by fuel vapour pressure and bond-gas pressurization, without involving any process of rapid sodium vaporization.

E- and H-Tests. These tests were carried out in the Mark-II flowing sodium loop with masses of fuel ranging from about 70 gr (1 pin) to 490 gr (7 pins). The thermal energy given to the fuel during the overpower transient ranged from 1500 J/gr to 3000 Joule/gr. Fresh and irradiated fuel pins were tested. The measured sodium temperature in failure region was from 500°C to 960°C. The earlier experiments (E2, E3, H2 and E4) simulated burst conditions characteristic of a start up accident (i.e., fuel initially at low power prior to the burst). The other tests (H5, E6 and E7) simulated, instead, reactor operating conditions. The energy conversion ratio was always very low (less than 10^{-3}).

Loss of Flow Transients. Two different test vehicles are currently being used to study failure consequences arising from complete loss of flow without reactor shutdown. The L-series tests (3 tests with 460 gr of fuel) are using the Mark-II loop while the R-series tests (2 tests, one with 180 gr and the second with 1270 gr of fuel) are being executed in the R-series test vehicle, which allows one to accomodate fuel pins having the same length as the FFTF pins. Test L2 was run with seven short fresh pins, while L3 used seven short pins irradiated at power levels insufficient to produce a well-defined central void, and the L4 sample consited of seven short pins irradiated at power levels high enough to produce a well-defined central void.

R3 was run with a single full length FFTF fuel pin. Again, only mild fuel-coolant interactions could be identified in either of these four experiments. This is consistent with the anticipated loss of flow sequence where molten fuel is produced at a time when sodium is out of the fuel zone and not likely to reenter because of a combination of clad plugging and sodium vaporization from hot steel at the axial extremes of the test section. Eventually local contact will occur, however, between liquid sodium and fuel. This will lead to nucleate boiling which will provide sufficient vaporization and therefore prevent coherent mixing between fuel and the liquid sodium.

2.1.2 RCN-Tests (Petten-Holland) (Ref. 8)

The RCN experimental programme on Fast Reactor Safety consists of irradiations of single fuel pins in a sodium environment under loss of cooling conditions. The irradiation programme consits of 17 experiments. The parameters are:

1. The time interval between the interruption of the cooling and the reactor scram (Loc-time)
2. The internal gas pressure of the fuel pin for unirradiated fuel
3. The burn-up for the pre-irradiated fuel pins.

The fuel pins consist of 5.1o mm diameter, 8%-enriched, UO_2-pellets with a stack length of 25o mm and clad in 5.24 mm inner diameter tubing, with a wall thickness of o.38 mm.
So far eight experiments have been performed with non pre-irradiated fuel pins. Two of these pins were pre-pressurized. The fuel stack of the non pre-pressurized pins failed after a Loc-time lasting longer than about 8 seconds. Fuel failure occurred after significant bulging mainly in the lower half of the fuel pins.
Fuel ejection, which happened quite slowly, was preceeded by sodium expulsion from the annulus, so direct FCI did not take place. Even more important was that also during sodium reentry a violent FCI did not take place.
Preliminary results of experiments with pre-pressurized fuel pins revealed that gas blanketing after pin failure under loss of cooling conditions can be rapidly followed by molten fuel ejection, however, without causing measurable pressure pulses.

2.2 Out of Pile Tests

Table 1 gives a list of the out of pile tests in sodium with UO_2.

2.2.1 CEA Experiments (Grenoble-France (Ref. 1)

JEF Experiments. These experiments simulate a slow power excursion. Small quantities of UO_2 (few grams) are heated by means of Joule effect. UO_2 and Na are separated by an electrical and thermal insulator (alumine) of tubular form and by a stainless steel sheath. The only variable parameter is the Na temperature. Pressure and mechanical energy transmitted to the column are measured.
Measured pressures did not exceed a few atm (2 or 3). Fragmentation of UO_2 was very extensive.

Fragmented mass of UO_2 never exceeded 5o% of the total mass. A considerable part of the debris had the size of 1-2 μ.

CORECT 1 Experiments. 3oo gr of Na at 4oo°C were injected into 3.2 kg of molten UO_2, which was heated by high frequency in a crucible. Interaction conditions were not realistic. The pressure of the filling gas in the containment vessel was measured. In a typical experiment the pressure went up to 9.8 bars in 0.5 sec. Only 3oo gr of fuel were scattered around and only 3 gr were fragmented in particles ranging from 1 to 1oo μ. The crucible was deformed by the sudden formation of steam. The deformation of the crucible and the relatively high rate of the pressure build up in the containment vessel indicate that high pressures were produced inside the UO_2 due to the thermal interaction.

CORECT 2 Experiments. These experiment will simulate the interaction in an assembly under a sodium head as a result of melting of the fuel.
Experiments will start in 1974.

2.2.2 GfK Experiments (W.-Germany) in cooperation with C.C.R. Euratom Ispra (Ref.2)

It is basically a "shock tube" experiment with large quantities of UO_2 (5 kg). A tungsten crucible containing the molten UO_2 falls through a long vertical guide tube in an inert gas atmosphere. Immediately after, a large amount of Na is injected into the top of the reaction tube. Provisions are made to allow injection of small quantities of Na in UO_2 prior to the contact between the UO_2 and the large mass of Na. Experiments are expected to start in 1975.

2.2.3 PNC Experiments (Japan) (Ref. 3)

A series of 3o experiments were performed to examine the fragmentation characteristics of sodium-fuel interaction by dropping molten UO_2 into sodium. In this experiment, annular UO_2 pellets were heated by means of a central tungsten rod, and the molten UO_2 droplets fell into the sodium tank. The fragmentations of the droplets on the surface of liquid sodium were photographed with high speed camera at 5oo-2ooo pictures/sec. The pressure and temperature of the sodium tank were measured.

The particle characteristics of the UO_2 residue were examined: the particle size distribution, the particle surface condition, and characteristics of the grains. These examination indicates that the UO_2 particles can be assumed to be spherical and to have the log-normal distribution function.

The most pessimistic particle size distribution at present can be represented by the equation

$$f_i\ (D) = 2.317 \exp\left(\frac{-(\log D - 2.267)^2}{o.9442}\right)$$

where $f_i\ (D)\ dD$ = weight percent of particles in size range D to D + dD, with "D" being given in "μ".

2.2.4 CNEN Experiments (Italy) (Ref. 4)

AF2 Experiments. These experiments are similar to the french JEF experiments. Small quantities of UO_2 (5o gr) are heated inside a stainless steel clad by means of the Joule effect. The insulation material is boron nitride. In a typical experiment two pressure pulses were recorded: the first of about 6 bars and the second of about 22 bars after 2.3 secs. It is believed that the molten UO_2 increases in volume in such a way, that a jet of UO_2 was formed perforating the clad and determining the first pressure pulse and vapour formation. A vapour recondensation with liquid sodium entering the pellet may have happened. This should have produced a second interaction with Na vapour driving out other molten fuel. Not all the molten UO_2 escaped from the clad but an outer annulus remained in place and recrystallized. The debris was only 5 gr with dimensions ranging from few microns to few millimeters.

AF 4 Experiments. They will be carried out in a test-rig similar in principle to that of the AF2 tests, but with some additional modifications. Provisions are made to test a 7 pins cluster. The starting date for these experiments is not given in the paper.

2.2.5 ANL (USA) (Ref. 5)

Small Scale Drop Experiments

Masses of UO_2 ranging from 8 to 3o gr were dropped in a volume of 3oo cm^3 of Na at a temperature ranging from 2oo°C to 6oo°C. Extensive fragmentation of UO_2 was observed but no relevant pressure pulses were measured. Similar results were obtained by dropping stainless steel at melt temperature into sodium.

Small Scale Injection Experiments

Small volumes (1o cm^3) of Na were injected in molten UO_2. In most of the cases a violent interaction was observed. The vapour explosions occurred with a delay of 9 to 3oo msec after the time of injection. Upon initial contact, sodium vapour and droplets spewed out of the top of the crucible in a relatively mild manner. However, data recorded from pressure and force transducers and from the high speed motion pictures both indicate that violent interactions took place. A blast microphone located about 15 cm above the open top of the UO_2 crucible measured shock pressure pulses in the helium atmosphere ranging from o.3 to o.5 atm.

Large Scale Drop Experiments

Masses of UO_2 up to 3 kg were dropped in a Na-pool. The UO_2 at a temperature between 55oo and 58oo°F was produced by a thermite-type reaction between uranium metal and MoO_3 with a small amount of CrO_3 which acted as an accelerator.
Extensive fragmentation took place but the interactions were relatively mild. Sharp pressure pulses (low energy content) were noticed.

2.2.6 CCR Ispra (Euratom)

Tank Experiments (Ref. 6)

These experiments are essentially similar to the ANL large scale drop experiments. The UO_2 is molten in a crucible by means of a radiation furnace. The results are consistent with those of the ANL large scale tests, that is, extensive fragmentation of UO_2 were observed and very low pressures were measured. Similar results were obtained by dropping stainless steel into sodium.

Channel Experiment (Ref. 9)

A sodium column was dropped above few grams of Al_2O_3. A low energetic pressure pulse of 7 bars was measured. Fragmentation occurred.

2.2.7 AWRE Foulness (Great Britain) (Ref. 7)

Pyrotechnic charges were used to melt and dispers UO_2 inside a pool of Na. The pressure pulses measured in the gas blanket (from 1 to 4 atm) seem to be due to the water vapour contained in the charge. Results with dried charges were not yet available, but they will be soon available in the next future.

2.2.8 Windscale-UKAEA (Great Britain) (oral announcement)

Shock tube experiments are foreseen to be carried out in 1974. They will use masses of UO_2 of the order of 5o gr. and volumes of Na of the order of $1o^3$ cm^3.

2.3 Simulation Experiments

Some experiments were also carried out in water, which is much easier to handle than sodium and which has the great advantage of being transparent so that the thermal interaction can be investigated also with the help of high speed photography. The results of these experiments cannot be used in the case of sodium because of the different thermophysical properties of the two fluids. However, they can be of help in better understanding of the phenomena which occur due to the thermal interaction.

2.3.1 Al/Water Shock Tube Experiments at AWRE-Foulness (Great Britain) (Ref. 7)

Twentyfive tests were carried out with Aluminium initial temperature ranging from $66o^oC$ to $85o^oC$. Many impacts (a maximum of 4) were observed for each test, and pressure pulses in the water column were measured from 5o to 6oo atm. Most of the maximum peak pressures were obtained at the second or third impact, only two occurred at the 4th impact and none at the first impact. Correlations between measured pressures and Al temperature are difficult to be found because of the relatively poor reproducibility which has been achieved until now. The correlation between measured pressures and Al particles size is, instead, easier to be detected: the more energetic the interaction, the smaller the debris.

2.3.2 CEGB Experiments (Great Britain) (Ref. 1o)

Three types of experiments were carried out

Pressure Driven Blanket Collapse

To investigate the effect of rapid vapour-blanket collapse, about 6o grams of molten tin at 8oo^{o}C was poured on to a shallow crucible under water at an external pressure of 1oo$_{T}$. The vapourblanketed tin drop was then subjected to a rapid increase in pressure (1 bar in o.5 ms) by rupturing a diaphragm connecting the apparatus to atmosphere. Pressure in the vessel was measured and events were photographed at 8ooo ps^{-1}.

The results showed that vapour-blanket collapse occurs within 1 ms of diaphragm rupture, and an explosion occurs within the next two frames of the film (o.25 ms). A typical pressure trace shows that the explosion pulse is 4 bar x 1 ms, and that there are no other events of significance either before or after the main pulse. The experiment was repeated using aluminium, and a similar though less vigorous explosion was obtained, thus confirming that the interaction was caused by the violent collapse of the blanket.

Experiments with a long crucible

The previous experiment indicated that explosion propagation through blanket collapse was energetically plausible. To test whether propagation would actually occur in practice, an experiment was designed in which about 2oo grams of molten tin were poured into an aluminium crucible 3o cm long and of shallow "V" cross-section, immersed in an open tank of water at 8o^{o}C. The instrumentation consisted of 3 pressure transducers immersed in the water 1o cm above the crucible and spaced along its lengths and 5ooo ps^{-1} cinephotography.

At low tin temperatures (65o^{o}C) a spontaneous interaction occurred (unexpectedly) near one end of the crucible. This was probably due to transition boiling. At higher initial temperatures (75o^{o}C) there was no spontaneous interaction and so the interaction was initiated by applying an impulse to one end of the crucible via a steel rod.

In general, whether the interaction was spontaneous or induced, the results showed that the initial event was weak and localised (at the lefthand end) and escalated in a single vapour growth-and-collapse cycle to a vigorous but still localised interaction. Subsequent events, however, did not proceed through growth and collapse in this manner. During the growth phase of the "bubble" from this first vigorous interaction a second interaction occurred 1o-15 cm away, near the center of the trough, and during the growth of this latter region a third interaction occurred at the right-hand end.

The time interval between the successive interactions was typically in the range of 2-5 ms and the effective propagation velocity was 3-8 x $1o^3$ cm s^{-1}. The pressure pulses recorded from individual interactions were relatively low (o.7 bar) but of long duration (3 ms). When subsequent interactions occurred within this pulse width, however, the pressures combined additively so that some resulting pulses were both higher (up to 1.5 bar) and longer (up to 1o ms).

Thin tank experiment

To increase the dynamic contraint to that which would be experienced by a full-scale explosion occurring at the horizontal interface between large regions of molten metal and water, a tank was constructed which was submerged in a large vessel containing water at $8o^oC$. About 2oo grams of molten tin at $7oo^oC$ were poured into the tank and an interaction was initiated by tapping the base near one end. The high-speed film record, taken together with the pressure trace showed that the initial perturbation produced only a very minor splashing interaction confined to the left-hand end of the tank. About 1o ms after this, however, a vigorous explosion begins in the splashed tin and propagates rapidly along the tin/water interface, travelling 15 cm along the tank in 3 ms before the pressure drops. The apparent propagation velocity is 5.1o^3 cm s^{-1}.

Conclusions

The conclusions of these experiments given by the authors are the following:

1. The results of several small-scale experiments demonstrate that spatial propagation (autocatalysis) can occur in thermal explosions.
2. The results also suggest that the observed explosions are primarily due to fragmentation rather than superheat.
3. It is shown that propagating fragmentation or mixing can occur through self-driven blanket collapse. At least some of the mixing may be due to the penetration of coolant jets formed by the collapse of vapour domes in the blanket.
4. In a continuously propagating explosion, however, Taylor and Kelvin-Helmholtz induced mixing due to the motion of the interaction region could become the dominant process.
5. There is some evidence that the propagation velocity is associated with sonic choking in the 3 phase interaction region.

2.3.3 Small scale drop experiment at Culham UKAEA (Great Britain) (Ref. 11)

These experiments are somewhat similar to some others previosuly reported by the CEGB (ref. 24). Small quantities of Tin (few grams) were dropped into water. Water temperature ranged from 1o to $9o^oC$ and tin temperature from 25o to $9oo^oC$. The main results were as follows:

1. High speed photograms show that in all experiments there is a multiple set of interactions with increasing intensity, characterized by the growth and collapse of vapour bubbles
2. The "dwell time" (that is the time between the metal first entering the water and the initiation of the explosive interaction) increases with "Sn" temperature.
3. The percentage disintegration "PD" (that is the ratio of the fragmented mass of fuel to the total mass) increases with "Sn" temperature
4. A threshold temperature " Θ_{th}" exists. The interaction occurs only if the water temperature is lower than this threshold temperature.

The explanation for this threshold temperature given in ref. 11 is the same as that given by the author in a previous publication (ref. 25). Stable film boiling (which hinders liquid/liquid direct contact) occurs when the fuel surface temperature "T_f" is higher than the minimum fuel surface temperature " Θ_{min}" for stable film boiling ($T_f > \Theta_{min}$).

Since " Θ_{min}" is a function of the bulk temperature " Θ_b" of the cold liquid (fig. 3) the above condition can be expressed by the equivalent condition $\Theta_b > \Theta_{th}$, where " Θ_{th}" is the liquid coolant bulk temperature at which $\Theta_{min} = T_f$. In a previous experiment (ref. 24) it was shown that interaction can take place also for temperatures $\Theta_b > \Theta_{th}$ (that is $T_f > \Theta_{min}$, Region 2 in Fig.3) by breaking the stable vapour film with an external mechanical disturbance.

2.3.4 Small scale drop experiments at Karlsruhe (W.-Germany) (Ref. 12)

Interactions between single drops of molten metal and water were investigated with the following metals: Ag, Au, Cu, Pb, Sn, Zn, and Stainless Steel. Individual metal particles of metal, of about 0.5 grammes, were heated by means of electrical induction in a levitation coil to a temperature above their melting point. Next, the molten metal particle was dropped into a small plexiglas vessel with 10 to 50 cm^3 of cold water. The temperature of the particle was measured by a thermocouple located in the center at the bottom of the vessel which penetrated into the particle.

The phenomena in the interaction zone could be observed and filmed, and simultaneously the temperature of the metal particle at the bottom of the vessel was registered.

The following parameters were varied in the experiments:
"the initial temperature" of the particle, the distance between the levitation coil and the plexiglas vessel, the diameter of the vessel, the volume and initial temperature of the water. The geometry of the interaction zone was also varied. Some experiments were made in inert gas atmosphere (argon or N_2).

Thermal explosions appeared under special precisely determined conditions, and it seemed to follow after the direct contact of both hot and cold liquids. For the copper/water interactions, the thermal explosion occured for two specific initial temperatures of the copper particle in the levitation coil: 1400 ^{o}C (levitation time 6 sec) and 1600 ^{o}C (levitation time 10 sec). In the first case the explosion occurred just below the water surface, and in the second case at the bottom of the vessel. A delay of about 1.5 to 5 ms was observed between this direct contact and the thermal explosion. The temperature measurements before and during the thermal explosion at the bottom of the vessel showed that the collapse of the vapor film happened with copper/water combination at the temperature of 1300 ^{o}C. After that, the temperature of the copper particle dropped very rapidly to the temperature of 1022 ^{o}C, which is the solidification temperature.
The explanation of these results is still debatable. The author of Ref. 12 suggests that fragmentation is due to the rapid solidification of the molten metal after direct contact with the cold liquid has occurred.

2.3.5 Visualization of boiling following direct contact between hot and cold liquid (CEA Grenoble-France) (Ref. 13)

Thermal interactions between a small volume of cold water (1 cm^3) and a bath of hot oil under various conditions were filmed by means of a high speed camera.

Heating of the cold liquid by direct contact

A quantity of 1 cm^3 of water was injected into the oil at 250 ^{o}C in a fraction of a second. The water reached the boiling point and caused the oil to boil creating a whitish froth. There was no explosive reaction.

Heating of the cold liquid enclosed in a non rigid envelope

To allow the introduction of a volume of 1 cm^3 of cold water into the oil in a single move, a non rigid envelope was obtained by enveloping a ball of ice with paraffin. Once the ice melted, the ball was plunged into the oil at 250°C. The same phenomenon as previously was observed. There was no explosive reaction.

Heating of the cold liquid enclosed in a rigid envelope

a) With no air

A ball made of glass was filled with water. Care was taken to ensure that no air was contained in the envelope.
The ball was plunged into the oil at 250°C. After approximately 15 seconds, dilation of the water caused the ball to break. Rapid ebullition with formation of a whitish froth was seen. There was no explosion.

b) With air

The ball was partially filled with water, but a certain volume was occupied by air. The ball was plunged into the oil at 250°C. After a delay time varying between 1 to 3 minutes, the ball exploded. Oil was projected violently.

Heating of the enclosed cold liquid by hot air

The ball was heated up to 200°C by blasted hot air. There was an explosion.

2.3.6 ANL Experiments (USA) (Ref. 14)

To test the criterion of Fauske (see section 4) for vapour explosion, experiments were carried out with saturated Freons and oils and water as hot liquids. These experiments included contact temperatures below (case 1) as well as above (case 2) the spontaneous nucleation temperature of the more volatile liquid. In case 1 no vapour explosion occurred. In case 2 instead a vapour explosion occurred.

3. Review of the parametric models described in the papers presented at the Ispra conference

A comparison among different codes was carried out by calculating a test case (ref. 15). All the models are characterized by a Phase A in which the sodium remains liquid and a Phase B in which vaporization takes place. The main features of these models are given in table 2. Results for phase A were consistant and differences could be explained. For phase B the results of only three models could be compared (Syremalensios, Caldarola and Scarano) and the differences among the various results could not be fully explained, because the postulated heat transfer mechanisms were quite different.
Extensive parametric studies were carried out based basically on the ANL parametric model with inertial constraint (Ref. 16). The conclusions of these calculations were as follows. Noncoherence in the interaction results in reduction in mechanical work. For the expected range of realistic mixing times, however, the reduction in work is small.
Estimated reduction in calculated mechanical work resulting from reducing heat transfer in proportion to the volume fraction of vapor is not large (about 20%). Cutting off heat transfer completely at the start of saturated boiling results in larger reductions; although early cutoff has not yet been demonstrated, this result shows the incentive to study the possibility of stable film boiling even while the bulk sodium is still subcooled.

The use of the single mass median diameter to represent a distribution of fuel particle sizes is an adequate approximation. The calculated work based on inertial constraint calculations did not rise as high as expected for small particle sizes.
Heat transfer by condensation of sodium vapor on the cladding of the fission gas plenum leads to reduction in mechanical work, but a better treatment is needed before the extent of this reduction can be evaluated.
Preliminary calculations were also carried out with the japanese code "Sugar" (Ref. 17) which is based on the FCI-ANL parametric model. This code accounts also for the deformation of the surrounding structure materials. It was concluded that the results were not realistic.
The Sugar-code will be modified with more practical and appropriate models based on experimental results.

A first attempt to incorporate a fragmentation model in the description of the FCI has been done in Ref. 19. Here fragmentation is due mainly to two effects: solidification process in the fuel and impact of the column of liquid sodium against the fuel. Numerical evaluations seem to agree with experimental results. However, the number of parameters in the code must be reduced in order to be sure that the agreement is not due just to a good choice of the numerical values of the many parameters.

4. Discussion of the experimental and theoretical results

4.1 Conditions for vapour explosion

Experimental results with UO_2 and sodium show that UO_2 fragments extensively and that no energetic interaction occurs except in the case where a few grams of sodium were injected in UO_2. This means that there is nothing inherent in these materials to prevent an energetic interaction on a small scale. However, in order to produce high efficiencies, a single coherent interaction on a large scale must occur, and this was never observed in all the experiments which have been carried out until now.
Energetic interactions as well as fragmentation of the hot material were instead produced in other systems such as Al/H_2O or Sn/H_2O.
The mechanism of thermal explosion may be explicable either in terms of the rapid release of energy stored as superheat in the cold liquid (explosion due to superheat) and/or as a rapid energy transfer and simultaneous release occurring because of an associated rapid mixing process (fragmentation explosion).

A. Explosive boiling due to superheat requires that the following conditions are satisfied (Fauske Ref. 14).

1. Direct liquid-liquid contact (or solid-liquid contact)
2. The temperature of the hot liquid must be equal to or exceed the spontaneous nucleation temperature "Θ_h" of the cold liquid
3. If the contact temperature Θ_c at the instant of contact is less than Θ_h ($\Theta_c < \Theta_h$) rapid heating is required in the presence of nucleation sites (solid-liquid systems). In the absence of nucleation sites (liquid-liquid systems) slow heating is sufficient. If "Θ_c" exceeds Θ_h ($\Theta_c > \Theta_h$) the effect of nucleation sites is not important.

If one applies these criteria to the UO_2/Na systems, one sees that $\Theta_c < \Theta_h$, which means that rapid heating is required in the presence of nucleation sites or that slow heating is sufficient if there are no nucleation sites. Since in LMFBR environments an ample supply of nucleation sites is generally available (gas bubbles, solids, fill gases, fission gases and fragments), molten UO_2 encountering liquid sodium will generally lead to nucleate boiling, where the vapour generation rate is many order of magnitude smaller than that associated with explosive boiling. Small-mass vapour explosions would be, however, possible when liquid sodium is entrapped inside molten UO_2. Due to the lack of nucleation sites (liquid-liquid contact) there will be overheating of the liquid sodium until spontaneous nucleation occurs. If we apply now the same criteria to systems

such as Al/H_2O or Sn/H_2O, we see that $\Theta_c > \Theta_h$. Large-mass vapour explosions are therefore possible. This has been observed experimentally. In the case of stainless steel/sodium systems the condition $\Theta_c \geq \Theta_h$ is satisfied for stainless steel temperatures of the order of 3000°C (well above the melting point). Stainless steel is present in a LMFBR core. However, due to the fact that there is no internal heat source, it is difficult to envisage situations in which such an high temperature can be reached unless a sudden and very fine intimate mixing among fuel, stainless steel and sodium is postulated. Experimental results don't seem to support this hypothesis. Instead they show that the cladding acts as a barrier which makes it more difficult for UO_2 to come in contact with sodium.

B. The conditions which must be satisfied in order to have "fragmentation explosion" cannot be stated as precisely as those for "explosion due to superheat", because the fragmentation process is not yet well understood. Many hypothesis have been postulated to explain the fragmentation process. They will be examined briefly. Here we can say that, whatever the fragmentation process is, the rate of particles coming in contact with the cold liquid must be high enough to produce vapour at such a high rate that it cannot be quickly releaved. This means that fragmentation must occur under mechanical constraint.

C. A third hypothesis may be that of considering the explosive boiling due to the superheat as the triggering mechanism leading to the sudden and very fine intimate mixing between molten fuel and coolant, which in turn causes the large explosion. This hypothesis has the advantage of satisfying the conditions of hypothesis A (which are based on clear experimental evidence) and at the same time of allowing to postulate an higher energy density of the explosive yield , which can be more easily explainable by means of hypothesis B (fragmentation explosion) than by means of hypothesis A (explosion due to superheat). We may call this hypothesis "fragmentation explosion triggered by homogeneous nucleation of the colder liquid".

4.2 Description of various fragmentation mechanisms (Ref. 25,38)

4.2.1 The fragmentation mechanisms may be classified in the following categories.

A. Entrapment Fragmentation was demonstrated in the experiments of Long (Ref.26) involving the dropping of large quantities (50 lbs) of molten aluminium in water. This mode of fragmentation is induced by the evaporation of coolant entrapped between the hot molten material and a solid surface. In Long's experiments, when the entrapment of water was made difficult by greasing or painting the bottom of the water container, fragmentation of the aluminium was prevented.

B. Impact Fragmentation was demonstrated in the shock tube experiments of Wright (Ref. 27). In those experiments a column of water held in a tube impacted on hot molten metals at the bottom of the tube. Impact fragmentation has been attributed to the effects of the mechanical impact. Recently, the observed fragmentation and vapor explosions in shock tube experiments have been associated with spontaneous nucleation of the coolant (Ref. 28). The limited data available from shock tube experiments does not provide conclusive evidence for any of these proposed mechanisms of fragmentation. Lately Kottowsky (Refs. 9 and 19) suggests this hypothesis to explain his experimental results in the "channel experiments" in which Al_2O_3 was fragmented under a column of liquid Na.

C. Hydrodynamic Fragmentation was demonstrated in the experiments of Ivins (Ref. 29) involving the fragmentation of mercury in water under isothermal conditions. This mode of fragmentation is caused by the nonuniformity of the forces resisting the motion of a deformable body in a fluid. Hydrodynamic fragmentation is sometimes referred to as the Weber Number Effect since a critical Weber Number has to be exceeded if hydrodynamic fragmentation is to take place. This mode of fragmentation has been thoroughly analyzed by Hinze (Ref. 3o).

D. Fragmentation due to the rapid solidification process in the hot material

Fragmentation may be postulated to result from pressurization of the hot material due to shrinkage of the rapidly solidifying surface. Fragmentation due to rapid cooling of Al_2O_3 in argon atmosphere (Ref. 9) seems to validate the hypothesis of fragmentation due to rapid solidification.
In Ref. 41 it is shown that, for temperatures below the nucleation point, the net rate of solid growth as determined from crystalization theory may be few order of magnitudes higher than the rate of solidification determined from the heat transfer process. In the case of UO_2/Na systems the contact temperature is lower than the nucleation temperature, so that a rapid solidification process is possible. In Ref. 19 simple calculations in the case of a sphere of molten UO_2(at 28oo^oC) in a bath of sodium (at 6oo^oC), show that the internal liquid pressure due to the contraction of the frozen outer shell can be kept for a radius of the sphere up to o.1 μ. All fuel particles having a larger radius will be rugged on the surface. The model of Ref. 3 postulates the existance of three zones in a solidifying sphere of hot material, the internal being liquid, the intermediate being a visco elastic shell and the external an elastic shell. If the tangential stress in the elastic region exceeds the fracture stress, the fractures occur. At the time of fracture, if the internal pressure is high, extensive fragmentation will occur. Another possibility may be that of the formation of a liquid jet of the hot material at the time of fracture of the external shell due to the interal pressure of the liquid (Ref. 12).

Fragmentation would follow immediately afterwards.

E. Fragmentation due to the boiling process in the colder liquid (Ref. 25)

As shown in the diagram of fig. 1 fragmentation can occur due to one of the three following processes:

Process 1 Highly superheated coolant vaporizes so quickly, that an energetic high pressure pulse is generated, which fragments the fuel (Block A).
This high superheating may be caused, either istantaneously due to the fact that the liquid/liquid direct contact temperature "θ_c" is close to the homogeneous nucleation temperature "θ_h", or with a short delay because of the entrainment of coolant droplets inside the fuel (Fauske Ref. 32 and 33).

Process 2 Fragmentation is generated by vapour film collapse or by bubble growth and collapse (Block C and B). The coolant microjects, which are produced during collapse, may be shown to have sufficient kinetic energy to produce fuel fragmentation directly (similar to cavitation processes).

Process 3 The microjects may have sufficient energy to penetrate into molten fuel which leads to dispersion and entrainment of coolant droplets resulting in fragmentation as in process 1. This path (Blocks C; G; A) is initiated in the same manner as process 2 (vapour film collapse or bubble growth and collapse), but leads to the fragmentation process 1. This path was suggested by the English CEGB and by the Culham Laboratory (Ref. 24, 11).

To initiate these processes several conditions must be met. The following conditions are common to all processes (Fig. 1).

1. The temperature, T_f, of the fuel must be equal to or higher than its melting point, T_{melt} (condition 1)
2. A liquid/liquid direct contact must be established between the materials either with entrainment of coolant droplets into fuel (conditions 2A) or without entrainment (condition 2B). Process 2 can also be initiated by an initial vapour film (condition 5B).
3. The liquid/liquid direct contact temperature "θ_c" must be either higher than "T_{melt}", or lower than T_{melt}, but with a solidification rate for the fuel so low, that only a very thin and weak crust at the surface of the unfragmented fuel is allowed to form during the interaction (conditions 3'; 3"). In addition the following conditions apply for processes 1, 2 and 3.
4. Process 1 can take place also with liquid/liquid direct contact without entrainment, provided that the contact temperature θ_c is greater than the homogeneous nucleation temperature "θ_h" (condition 4A). As discussed by Fauske (Ref. 33) there is experimental evidence that rapid vaporization due to homogeneous nucleation produces a shock wave, which may cause fuel fragmentation.

5. Another necessary condition for the processes 2 and 3 is that the coolant bulk temperature "θ_b" must be lower than "θ_{sat}" (subcooled coolant) (conditions 4B; 5B).

Whichever process takes place, there will be fragmentation, enhancement of fuel surface available for new liquid/liquid direct contact, mixing of fuel with liquid and between cold and hot liquid, so that the coolant bulk temperature "θ_b" will increase.

The fragmentation process may be extended to the remaining mass of unfragmented fuel either by successive vapour bubbles growth and collapse (Ref. 24, 11) or by a spatial propagation mechanism due to a disturbance pressure wave in the 3 phase interaction region (Ref. 1o).

In the case of the UO_2/Na thermal interaction the following must be pointed out:

1. The liquid/liquid direct contact temperature "θ_c" is lower than the homogeneous nucleation temperature "θ_h" (Ref. 32), so that process 1 can only occur through the initial entrainment of the coolant droplets inside the fuel.
2. Since the high energetic pressure pulse of the injection experiments seem to be connected to the artificially induced entrainment of coolant droplets in fuel, and since no high energetic pressure pulse was observed during the dropping experiments, one should conclude that process 1 (Fig. 1) cannot be induced through block G.
3. A configuration of the type described by Hall and Board (Ref. 1o) is not realistic, because stable film boiling is not possible in the molten UO_2/Na systems. With reference to fig.3, stable film boiling occurs if the fuel temperature "T_f" is higher than the minimum fuel temperature "θ_{min}" for stable film boiling. This does not happen in the case of UO_2/Na systems for sodium temperatures below 77o^oC. For sodium temperatures above 77o^oC film boiling is possible. However, due to the rapid loss of heat it may well be that the fuel solidifies very rapidly. This point needs still to be investigated (sect. 5).
4. In an actual reactor configuration initial entrainment of Na droplets in UO_2 cannot be entirely excluded. This means that process 1 may occur only as a triggering mechanism.

Taking into account the above four observations the diagram of fig. 2 may be proposed to explain the fragmentation process in UO_2/Na systems. In this diagram a loop has been shown to account for successive bubble growth and collapse processes.

To validate this hypothesis, let us look at the experimental results of fig.4. Here the degree of fragmentation is shown of stainless steel in sodium as a function of sodium temperature.

The results show that there is a sodium temperature at which the fragmentation has a maximum. The reason for having a maximum can be easily explained. The potential energy of a bubble (available for fragmentation) increases with its maximum volume (V_{max}) and with the difference (Δp) between the ambient pressure and the saturation pressure corresponding to the bulk sodium temperature. Now "Δp" increases with subcooling while "V_{max}" decreases. This means that the energy has a low value both for high Na subcoolings as well as near to the Na saturation temperature. A maximum must therefore exist in between, and this is confirmed by the experiments of instable film boiling of Ref. 39. Here pressure pulses were measured in a pool of liquid sodium in which a sphere of Tantalum was immersed at initial temperatures ranging from 2785 to 4195°F. Heights of the pressure pulses as functions of sodium subcooling are shown in Fig. 9. The curve has a maximum for a sodium temperature equal to 1382°F.

4.2.2 Concluding remarks on the fragmentation mechanisms

We have seen that fragmentation may be due to different causes and that there are experimental results which support the various hypothesis. For this reason it may well be that more than one fragmentation mechanism takes place in the UO_2/Na systems. The question to ask is therefore which one is the most important fragmentation mechanism.
The author feels that "bubble growth and collapse" in the cold liquid and the "rapid solidification of the hot material" seem at the moment the most promising hypothesis, which could explain fragmentation of molten UO_2 in sodium. The experimental results of Fig. 4 seem to support the first hypothesis. However, the fact that many fragments of UO_2 in the drop experiments (Ref. 42) were angular and rough-surfaced, indicates that part of the fragmentation occurred in the solid state. In addition a long delay time (5o - 15o msecs) between the drop entering the pool and the pressure pulse was observed in the UO_2 drop experiment. In the case of the stainless steel drop experiments his delay was much lower (3 - 3o msecs). This may also indicate that the solidification process plays a role in the fragmentation of UO_2 in sodium.

4.3 Parametric models

The author has carried out some additional calculations with his parametric model which show that peak pressure and specific work (Joule/gr of fuel) during phase A greatly decrease with the fuel mixing time constant "τ_f".
The case calculated is the same as the "test case" of Ref. 15. The results are shown in Figs. 6, 7, 8 and 9. The meaning of the symbols are the following (Ref. 4o).

R_f = mean radius of the fuel particles = 117 μ

σ = mean deviation of the log normal distribution of particles size

φ = initial gas to fuel volume ratio

The mass of fuel "M_f" has been supposed to be a linear function of time from the initial time to $t = \tau_f$

$M_f = M_{f\infty} \frac{t}{\tau_f}$ for $t \leq \tau_f$

$M_f = M_{f\infty}$ = const for $t > \tau_f$

Two cases have been calculated:

1st case: Mass of sodium $M_{Na} = M_{Na\infty}$ = const

2nd case: $M_{Na} = M_{Na\infty} \frac{t}{\tau_{Na}}$ for $t \leq \tau_{Na} = \tau_f$

$M_{Na} = M_{Na\infty}$ for $t > \tau_{Na} = \tau_f$

Results show that a value of τ_f of only 5 msec reduces in the first case the peak pressure by a factor of 2o and the specific work (referred to the mass of fuel which participates in the interaction) by a factor of 1o.
In the second case the reduction coefficients are still larger: 27 for the peak pressure and 25 for the specific work. This shows that noncoherence results in important reduction in mechanical work for very realistic mixing time constants (5 msec). It must be pointed out that the authors's model is different from the ANL model used in Ref.16. In the ANL parametric model(Ref.44) the equation used for the heat transfer does not describe any particular mechanism of fragmentation and mixing. It is only a practical expression easy to use. Instead in the author's model the time history of each fuel particle has been considered starting from the time at which each particle comes into contact with the coolant. In addition the author of Ref. 16 uses the inertial constraint from the very beginning of the interaction. For phase B the author basically agrees with the results given in Ref. 16, that is, vapour blanketing stronghly reduces the specific work. Similar results were already obtained by the author in Ref. 35 by making use of a model for the heat resistance at the interface, which was based on experimental evidence (Ref. 36).
In Ref. 36 it was observed experimentally that hot metal fragments remained suspended above a cool liquid surface by vapour generation, a phenomenon there called the "inverse Leidenfrost phenomenon". A laser was used to heat up pure metal foils under water. The foils exploded into small fragments. The range of the fragment temperatures was from 15oo^{o}C to 3ooo^{o}C and their size less than 1 mm in diameter. "Particle moving within their bubbles were observed to bounce repeatedly from the bubble wall and were thus effectively trapped within the bubbles, finally ending in a stable position above the base of the bubble. The mechanism for this interaction between the particle and the liquid is the generation of vapour from the liquid at the bubble wall, which exerts

a force on the particle: the vapour is generated by both radiative heat transfer from the particle and thermal conduction across the layer between the particle and the liquid. The vapour generation support for the particle may be expected to continue as the particles cools down, until it falls to temperatures comparable with the liquid saturation temperature. At this stage the vapour film will become so thin that it may be expected to break down" (Ref. 36).

Fischer (Ref. 43) has carried out some calculations with a model which includes the Cho and Wright ANL model of Ref. 44 for the mixing between fuel and sodium and the author's model of Ref. 35 for the vapour blanketing during Phase B. The results (pressure as a function of time) are shown in Figs. 1o and 11. In Fig. 1o the case is shown of a very low mixing time constant ($1o^{-6}$ secs). In phase B the two results are shown with and without vapour blanketing. The difference between the two pressure curves is relatively small.

In Fig. 11 the case is shown of a more realistic mixing time constant (1o msecs). The following two important points must be noticed:

1. The pressure in phase A is much smaller than that of Fig. 1o (peak pressure = 12o atm against 3545 atm of Fig. 1o)
2. The pressure in phase B is almost an order of magnitude smaller than that of Fig. 1o, and the effect of vapour blanketing has become large.

This means that vapour blanketing has an effect only if it is associated with a mixing time constant. The reason for this is the following: In the case of a low mixing time constant the sodium has received already most of the heat from the fuel at the end of phase A. Vapour blanketing during phase B is therefore not effective.This may be seen from the values of the sodium (θ) and fuel (T) temperatures at the end of phase A. The difference $T - \theta$ was $66^{o}K$ in the case of Fig. 1o and $1387^{o}K$ in the case of Fig. 11.

The conclusion is that properly chosen parametric models with reduced degree of conservatism may well lead to produce more realistic results.

5. Areas for further investigations

The existing programs (both experimental and theoretical) seem to be quite broad, because they cover (all together) already a relatively wide spectrum of accident conditions, especially if one considers the fuel subassembly accidents. The situation is less brilliant if one looks at the whole core accident because all the experiments are modest in size and the geometry of these accidents less predictable. In conclusion the following suggestions can be done, which in the author's opinion are all equally important:

1. Experiments should be carried out in which many kgs of fuel are involved, to examine the effect of experiment size on energy release.

Particularly the type of accident examined by Long (Ref. 26) in the case of aluminium and water cannot be entirely excluded in the case of the molten core falling above the "core catcher". Long carried out experiments with 5o lbs of aluminium.

2. Different contacting modes between hot and cold liquid and various geometries must be investigated. Particularly the experimental results show that entrapment of liquid sodium within molten UO_2 is a potentially dangerous mode of contact. More experiments involving larger quantities of Na being entrapped in UO_2 should be carried out. The influence of geometry (many pins) as well as that of enclosure of gas should also be investigated. Theoretical models for the interpretation and extrapolation to reactor conditions of these experiments must be developed.
3. Experiments should be carried out with molten UO_2 and Na at a temperature above $77o^{o}C$ to verify that configurations of the type investigated by Board and Hall in the case of water (Ref. 1o) are really impossible for UO_2/Na-systems. These experiments were already suggested by the author in Ref. 25.
4. The effect of rate of energy given to the fuel pins under various burn-up conditions must be further investigated in particular with regard to whole core accident.
5. Efforts on simulation experiments should be continued to find out other possible types of contacts between hot and cold liquid and other ways of propagation of small scale interactions to generate large scale interactions. Theoretical work to understand fuel fragmentation should also be continued.
6. In the field of parametric models efforts should be continued to try to reduce the degree of conservatism. Possible areas of investigations are: noncoherence,fuel blanketing, heat losses from the interaction zone, presence of structure materials and a well simulated mechanical constraint.

For the sake of completeness it must be pointed out that at the CREST meeting in Ispra somebody suggested to investigate the system stainless steel/sodium with stainless steel at $3ooo^{o}C$. However, because of the arguments given in paragraph 4.1.A, this situation seems to be very very unlikely to happen in a LMFBR core. For this reason the author feels that these experiments deserve a degree of importance lower than the above mentioned 6 areas for further investigations.

6. References

Note: References from 1 to 23 are the papers presented at the CREST second specialist meeting on "Sodium Fuel Interaction in Fast Reactors".

1. M. Amblard, J. Costa, P. Syrmalenios
"Recent JEF and CORECT 1 Sodium/Fuel Interaction Results"

2. H. Beutel, K. Gast
"Large Scale FCI-Experiments in Subassembly-Geometry-Test Facility and Model Experiments"

3. H. Misuta, F. Hirabayashi, N.Yokozawa,
"Progress Report on the Molten UO_2 Drop Experiments"

4. M. Martini et al.
"Out of Pile Tests on UO_2-Pins"

5. H.K. Fauske, T.P. Speis
"UO_2/Sodium Interactions - Recent in and out of pile Experiments in the US and their Interpretation for Fast Reactor Safety"

6. H. Holtbecker, P. Schlittenhardt, E. Soma et al.
"Results of Thermal Interaction Tests for Various Materials performed in the Ispra Tank Facility"

7. K.I. Darby, J.N. Guest, R.C. Pottinger, J.M. Rees, R.G. Turner
"Progress at AWRE Foulness on the Al/water shock-tube and UO_2/sodium thermal interaction rig"

8. H. Kwast
"Some Observations on Fuel/Sodium Interactions after Irradiation of Single Pins under Loss of Cooling Conditions"

9. J. Lazarus, J.P. Navarre, H.M. Kottowsky
"Thermal Interaction Experiments in a Channel Geometry using Al_2O_3 and Na"

10. S.J. Board, R.W. Hall
"An explosion propagation mechanism"

11. D. J. Buchanan
"Fuel/Coolant Interactions - Small Scale Experiments and Theory"

12. W. Zyszkowski
"Experimental-theoretical Investigation of the Thermal Explosion"

13. J. Costa, Fabrega, Flamand
"Visualisation of the Boiling Phenomena accompanying the Direct Contact of a Hot Liquid with a Cold Liquid"

14. H.K. Fauske
"Mechanisms of Liquid/Liquid Contact and Heat Transfer Related to Fuel/Coolant Interaction"

15. R. Potter
"A Review of the CREST Comparison of Sodium/Fuel Interaction Computations covering Seven Methods"

16. A.P. Reynolds, C.A. Erdman, P.L. Garner, P.M. Haas, C.L. Allen
"Evaluation of Conservatism in the Analysis of Fuel/Coolant Interactions"

17. O. Kawaguchi, M. Tezuka, K.Suzuki, K. Nagashima
"Theoretical Model of the Molten Fuel/Coolant Interaction in the Core Melt-down Accident"

18. M. Martini et al.
"Basic Experimental Techniques for visualisation of the fragmentation process"

19. W. Großgut, H.M. Kottowsky, H. Holtbecker, J.Pandles
"On the Process of Thermal Interaction between Molten Fuel and Coolant"

20. H.E. Schins
"The Consistent Boiling Model for Fragmentation in Mild Thermal Interaction"

21. L. Caldarola, G. Koutsouvelis
"The Karlsruhe Variable Mass Model for the Description of the Fuel/Coolant Interaction"

22. H. Jacobs
"The Calculation of the Consequences of Sodium/Fuel Interactions with Allowance for Temperature Gradients in the Sodium"

23. M. Martini et al.
"Results with and Indications of Possible Future Refinements of the FUS-PEC-Code"

24. S.J.Board, C.L. Farmer and Poole,
"Fragmentation in Thermal Explosions"
CEGB-Report No. RD/B/N 2423, Oct. 1972

25. L.Caldarola and W.E. Kastenberg" A model and conditions for fragmentation during molten fuel/sodium interactions",2nd Intern. Conf. on Struct. Mechanics in Reactor Technology, Berlin 1o-14 Sept. 1973

26. Long "Explosion of molten aluminium in water - Cause and Prevention", Metal Progress 71, 1o7-112, May 1957

27. Wright "Kinetic Studies of heterogeneous water reactors", Annual Summary report 1965, STR-372-3o, TRW Systems, Dec.1965

28. Fauske "The role of nucleation in vapour explosions" Trans.Am. Nucl. Soc. 15 (2), p. 813, Nov. 1972

29. Ivins "Reactor development program progress report, Nov. 1967, ANL 7399, 162-165, Dec. 1967

3o. Hinze "Forced deformations of viscous liquid globules" App. Sc. Research A1., 263-288, 1948

31. Witte et al. "Rapid quenching of molten metals", ORO-3936-6, Aug. 1971

32. H. Fauske "On the Mechanism of UO_2/Na Vapor Explosions", ANS Trans. 15, No. 2, Oct. 1972

33. H. Fauske "Nucleation of Liquid Sodium in fast reactors", ANL, Internal Report

34. Armstrong and Cho "LMFBR Nuclear Safety Program Annual Report, ANL 7800 310 -358, July 71,

35. Caldarola "A theoretical model for the molten fuel-sodium interaction in a nuclear fast reactor" Nucl. Eng. and Design, Vol. 22, No. 2, Oct.1972, p. 175-211

36. Hall et al. "Inverse Leidenfrost phenomenon", Nature 224 (1969)

37. Jacobs - Bericht über das "Second Specialist Meeting on sodium-fuel interaction in fast reactors", unpublished

38. Kazimi "Theoretical Studies on some aspects of molten fuel-coolant thermal interaction", MITNE-155, May 1973

39. Farahat "Transient boiling heat transfer from spheres to sodium", ANL 7909-1972

40. Caldarola, Koutsouvelis "Theoretische Untersuchungen zur Brennstoff-Natrium-Reaktion (BNR)", Beitrag zum 4. PSB-Vierteljahresbericht 1973, Abschnitt 1236.1

41. Cronenberg "Solidification Phenomena and Fragementation", ANL-RDP-18,pages 7-19/7-21, July 1973

42. Armstrong, Testa, Reridan "Interaction of Sodium with Molten UO_2 and Stainless Steel using a Dropping Mode of Contact", ANL 7890, December 1971

43. Fischer "BNR-1, ein Rechenprogramm zur Beschreibung der Brennstoff-Natrium-Reaktion, unpublished

44. Cho, Ivins and Wright "Pressure generation by molten fuel coolant interactions under LMFBR accident conditions", Conf. on New Developments in Reactor Mathematics, Idaho Falls, 1971 (Conf. 710 302).

Table 1

Out of Pile Tests

Ref.	Lab.	Name of Exp.	Mass UO_2 (gr)	Sodium		UO_2-Movem.	Containm. for UO_2	Mechan. Constr.	Heat. Source	No.of Tests	Starting Date	Sodium Movement
				Vol.(cm^3)	Temp.(^oC)							
1	CEA Grenob. (France)	JEF	7		4oo-7oo	Static	Clad	Na head	Joule	15	-	Static
		CORECT I	32oo-49oo	3oo	"	"	Crucible		H.F.	5	-	Injection
		" II	7ooo	$1o^3$-$1o^5$	"		"	Na head		-	1974	
2	GfK Germany		5ooo	$8 . 1o^3$	3oo-6oo	Fall	Crucible	Yes	Rad.	-	1975	Fall and Injection
3	PNC (Japan)	Drop Exp.	2o	3o-2oo	2oo-3oo	Fall	Alumina Tube	No	Tung. heater	3o	-	Static
4	CNEN (Italy)	AF 2	1o	1o		Static	Clad	No	Joule	3	-	Static
		AF 4	1ox7	1ox7		"	"	Yes	"	-	?	"
5	ANL (USA)	Small Scale Drop Exp.	8-3o	3oo	2oo-6oo	Fall		No		6		Static
		Inject. Exp.	3o-5o	1o	4oo	Static	Crucible			12		Injection
		Large Scale Drop Exp.	3ooo	$1o^4$		Fall		No	Thermite reaction			Static
9	CCR Ispra (Euratom)	Channel Geometry	few gr.		45o-75o	Static	Crucible	Na head	Rad.	-	1974	Fall
6		Tank Exp.	3ooo	very large	5oo	Fall	"	No	Rad.	1		Static
7	AWRE Foulness (GB)			large	25o	Static		No	Pyrot. Mixt.			Static
	Windscale UKAEA (GB)	Shock tube	5o	$1o^3$				Yes			1974	Fall

Table 2

COMPARISON OF MAIN FEATURES OF FCI MODELS

(from Ref. 15)

Name of Model/ Author/Reference	Fragmentation	Heat Transfer	Hydrodynamics
Argonne Parametric Model Cho, Ivins & Wright. ANL 7919 Conf.-71o3o2 (Vol. 7), p. 25	Particle size distrib. assumed.Fragmentation & history time can be simulated by choice of heat transfer mechanism	Heat transfer always into liquid sodium (even if vapour is predicted).Options: (i) linear gradient transient conduct. (upper approxim.) (ii)Quasi steady state (lower approxim.)	Acoustical & inertial constraint change over on return of rarefaction wave advocated
Cadarache Model Antonakas	Surface area increaded by progressively dividing fuel sphere into 2 equal surfaces	Transient conduction which ceases when vapour first produces	Acoustical & inertial constraint, change over when vapour first formed
Karlsruhe Model II Caldarola Nucl.Eng.&Design, Vol.22,No.2, Oct.72 and Ref. 21	Fragmentation & mixing given functions of time log normal distribution of particle sizes	When no vapour present, exact solution of heat transfer in a sphere. When vapour present a detailed model determines film thickness. (This model is based on the results of the CEGB laser experiments)	Acoustical & inertial constraint, change over on return of rarefaction wave.
BRENDY I/II Jacobs Proc.Conf.Eng., Fast Reactors Karlsruhe,Oct.72, paper 3Sg	No fragmentation but conductivities for fuel & sodium are increased to simulate increased area of fragmentation	One dimensional conduction from fuel layer to sodium with effective conductivity	BRENDY I-One dim. Lagrangian compressib. dynamics BRENDY II-Additionally contains options for accoustic or inertial constraint
FUS-PEC 1/2 Martini & Scarano CREST Specialist Meeting, Febr. 72, Grenoble, paper 17	Single particle size assumed	Phase A pure conduction into liquid using polynomial type approxim. Phase B heat transfer into mixture of liquid & vapour.Coeff. varies with void fraction. (FUS-PEC 2 solidification of UO_2 taken into account)	Acoustic constraint with inertial constraint after return of rarefaction wave

Table 2 continues in the next page

Table 2 (continued)

Name of Model/ Author/Reference	Fragmentation	Heat Transfer	Hydrodynamics
Mizuta	Single particle size assumed	Forced convection model	Acoustic constraint with inertial constraint when vapour is produced
TOPAL Morgan Proc.Conf.Eng. Fast Reactors Karlsruhe, Oct.72, paper 38c	Separate model required	Heat input into coolant channel from separate calculation	1D compressible flow Lagrangian Code
COPFU Syrmalenios Rapp. CEA-R-4432	Distinguishes between fragmentation (large scale break up) and dispersion (small scale break up) on different time scales	Heat is transferred from fuel to liquid sodium in the interacting region. There is exchange of mass and heat between vapour & liquid which are not in equilibrium. The effective area for the heat transfer between liquid and vapour is put equal to the volume of sodium multiplied by "$J\alpha(1-\alpha)$" where "α" is the void fraction and "J" is an arbitrary coeff. Additional liquid coolant can enter the interaction zone.	Non-interacting liquid is taken as incompressible giving inertial loading

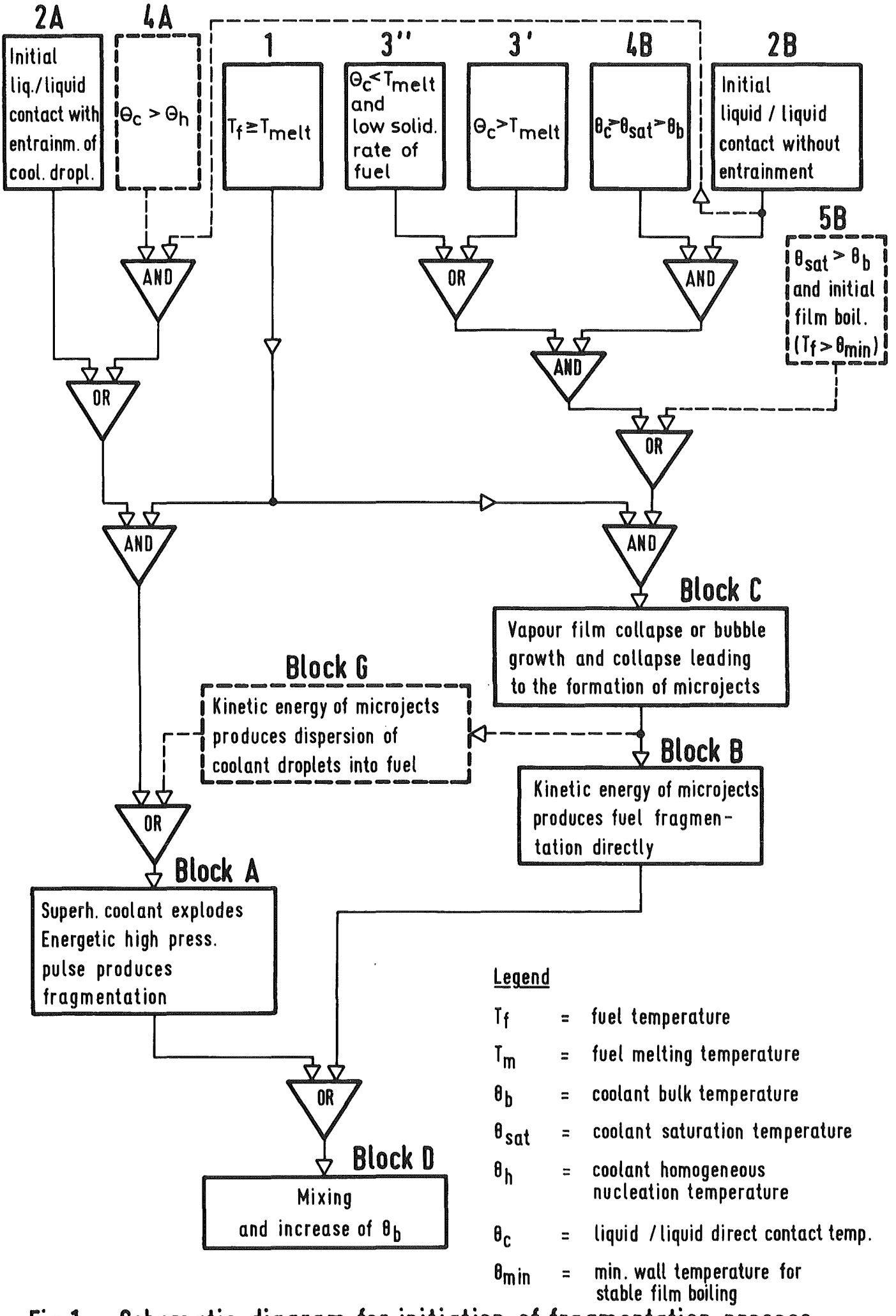

Fig.1 Schematic diagram for initiation of fragmentation process

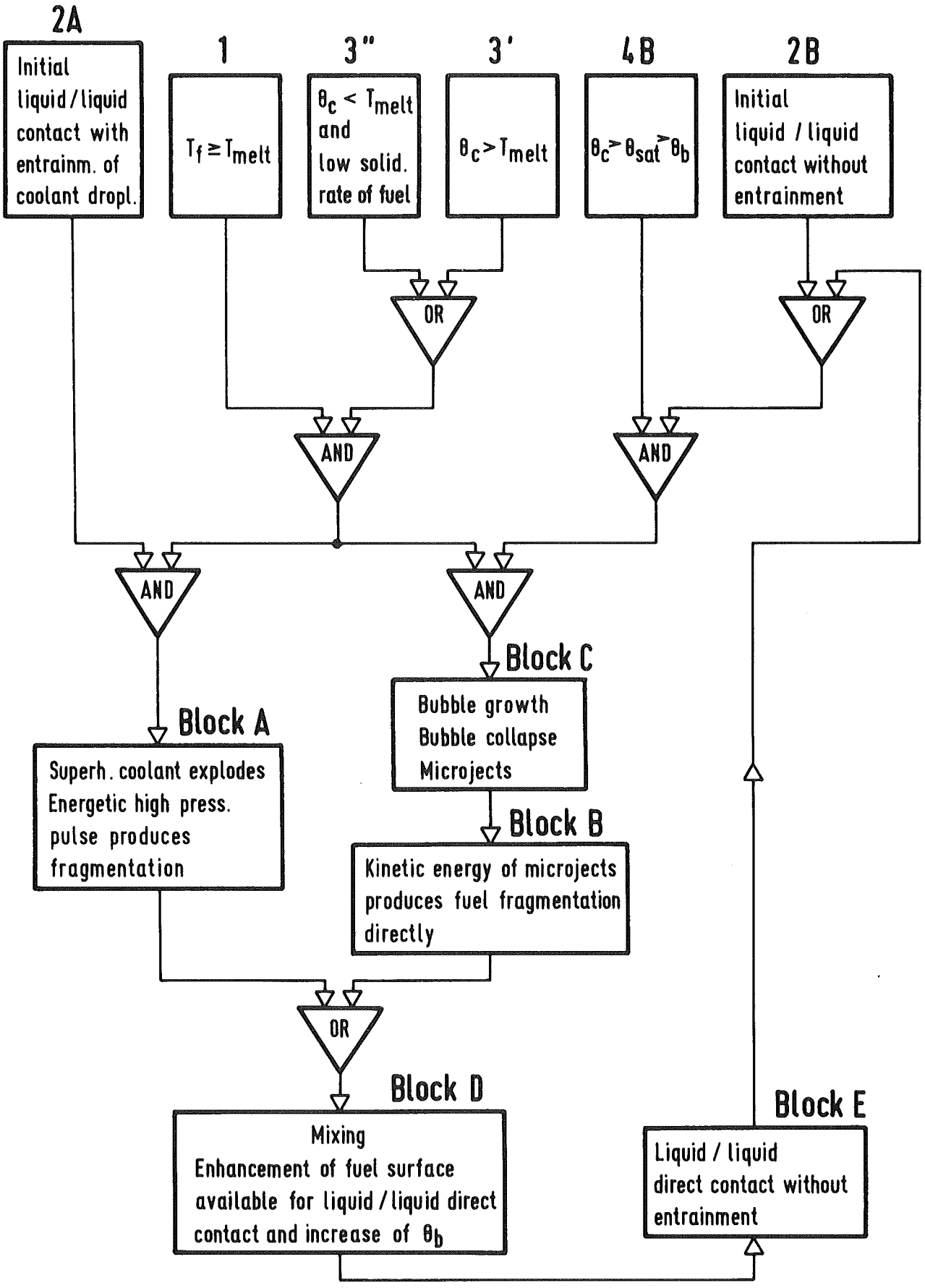

Legend

T_f	=	fuel temperature	θ_{sat}	=	coolant saturation temperature
T_m	=	fuel melting temperature	θ_h	=	coolant homogeneous nucleation temp.
θ_b	=	coolant bulk temperature	θ_c	=	liquid / liquid direct contact temp.

Fig. 2 Schematic diagram for fragmentation process of UO_2 in sodium

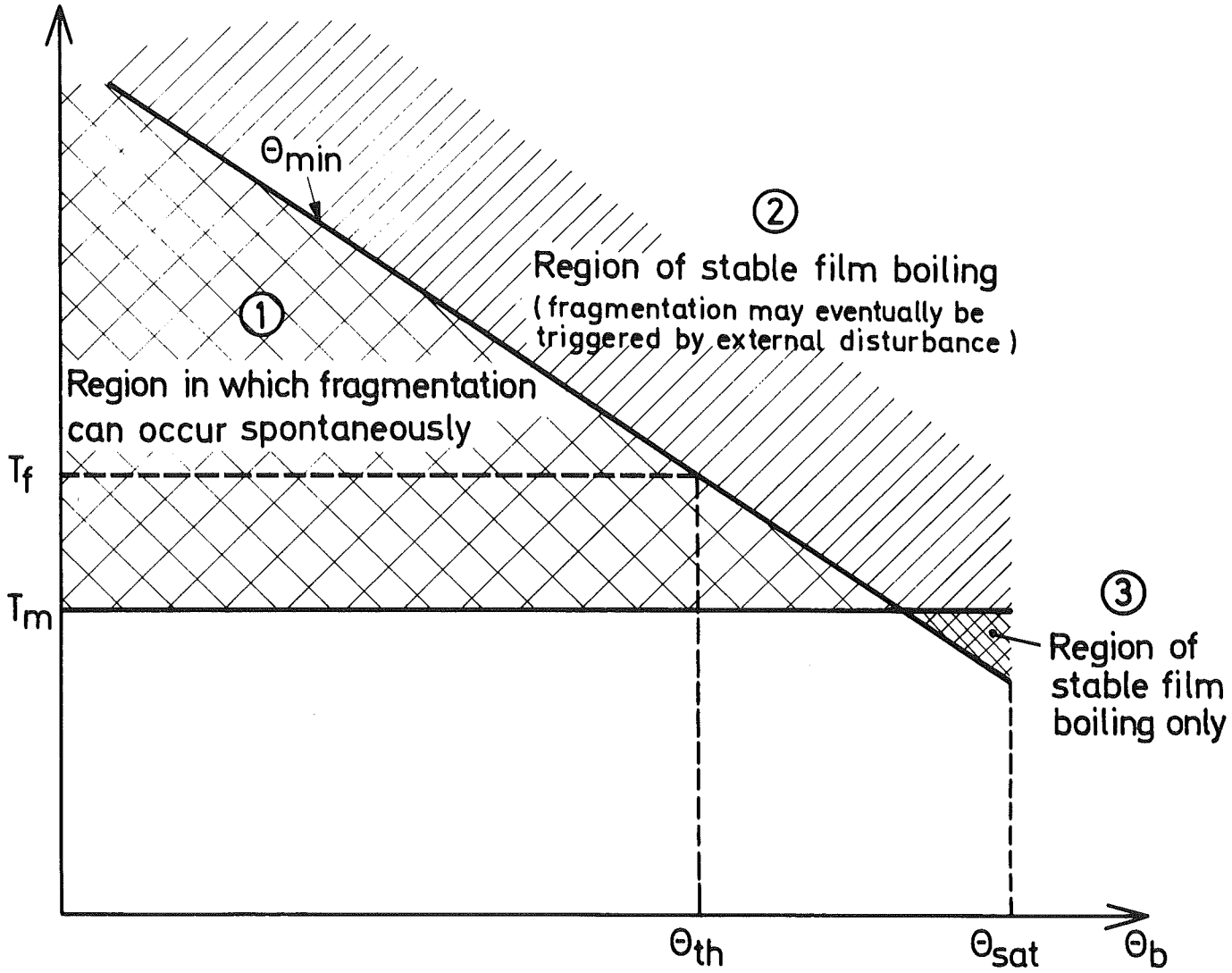

Condition for spont. fragm. to occur : $T_m \leq T_f < \Theta_{min}$

The condition $T_f < \Theta_{min}$ is equivalent to $\Theta_b < \Theta_{th}$

T_f = Fuel temperature

T_m = Fuel melting temperature

Θ_b = Coolant bulk temperature

Θ_{th} = Coolant threshold temperature

Θ_{sat} = Coolant saturation temperature

Θ_{min} = Minimum wall temperature for stable film boiling

Fig. 3 Definition of the regions of fragmentation and of stable film boiling

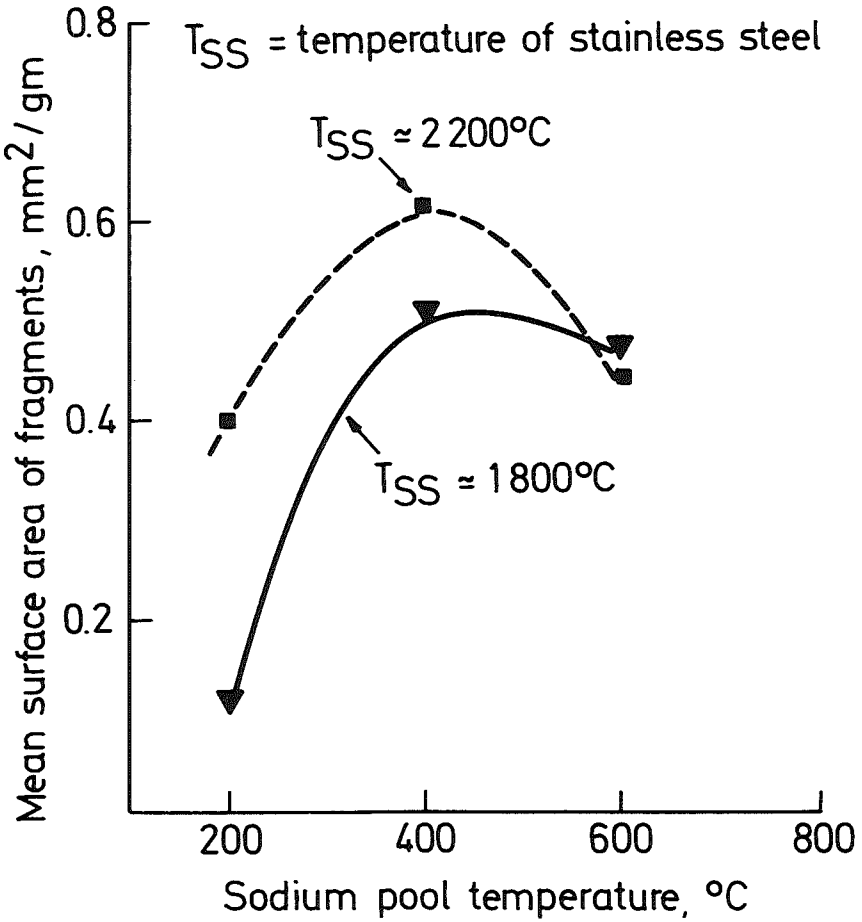

Fig.4 Results of drop experiments given in Ref. 38
(Area is based on mean diameter of fragments)

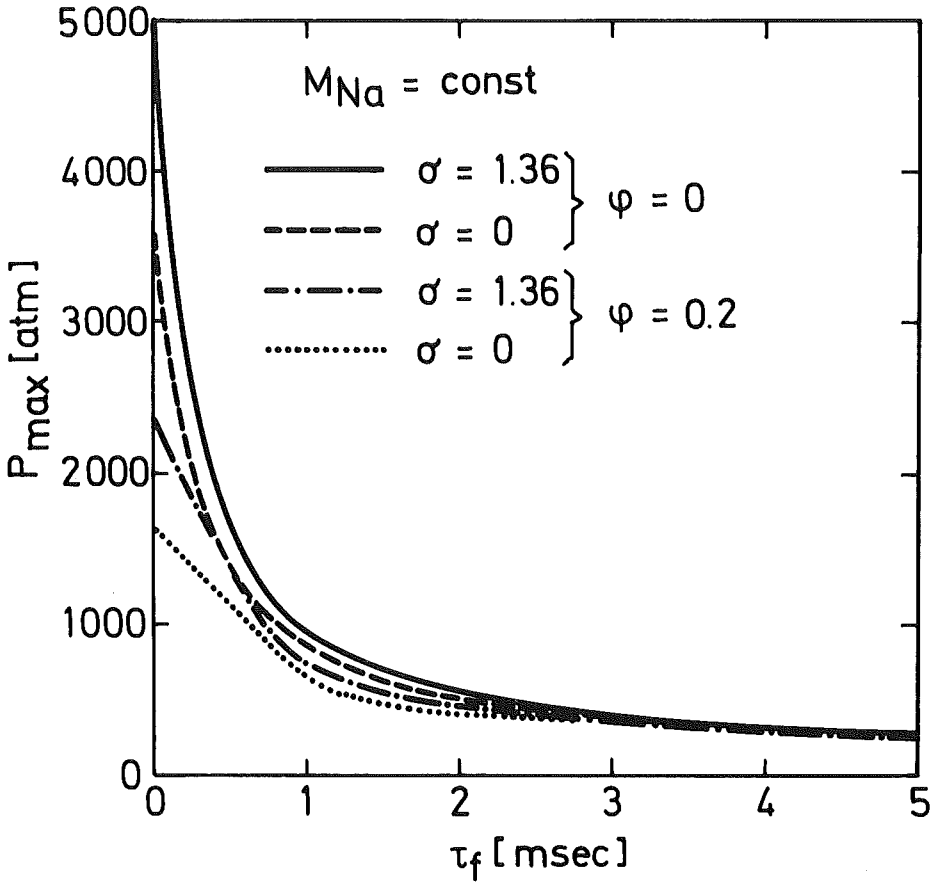

Fig. 5

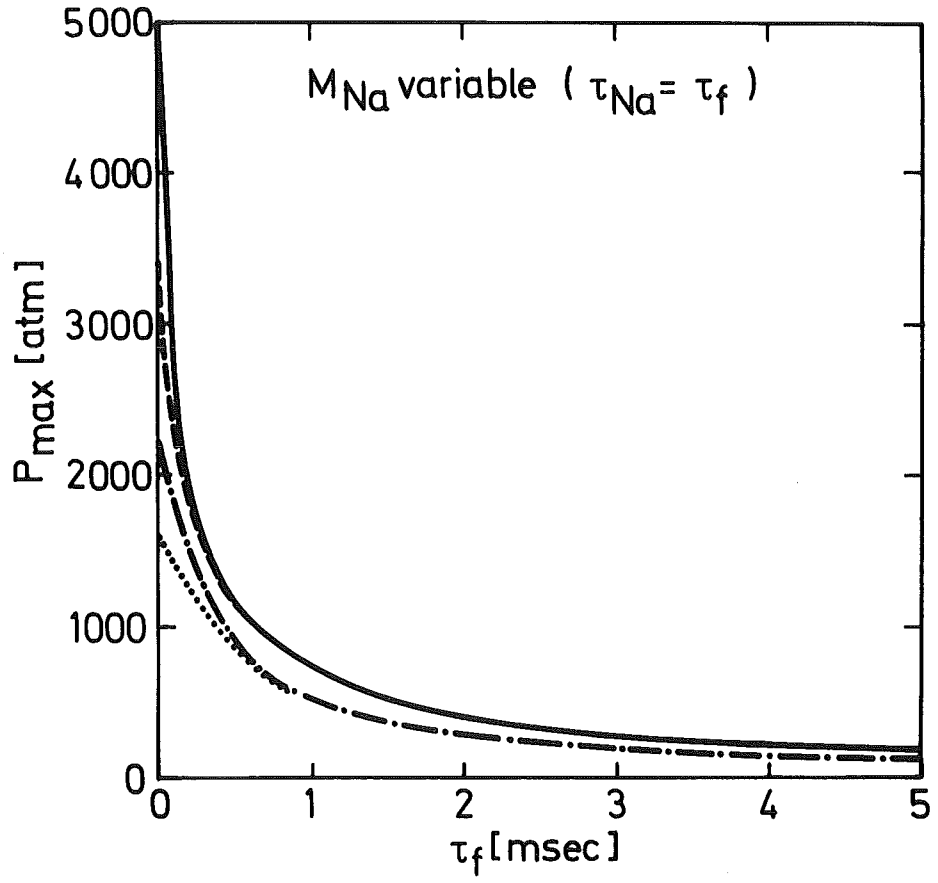

Fig. 6

Cho and Wright Case - M_f Linear Function of Time
Phase A - Peak Pressure as a Function of Fuel Mixing Time Constant

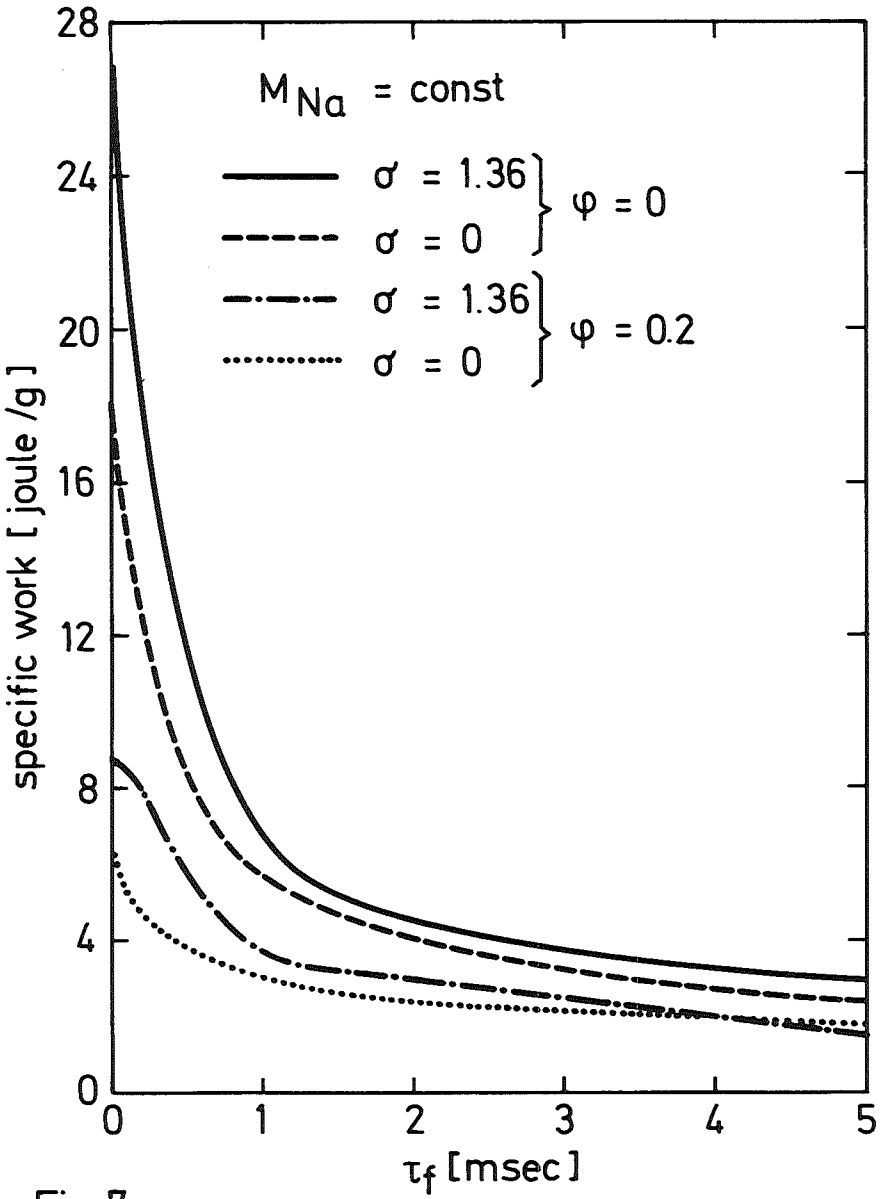

Fig. 7

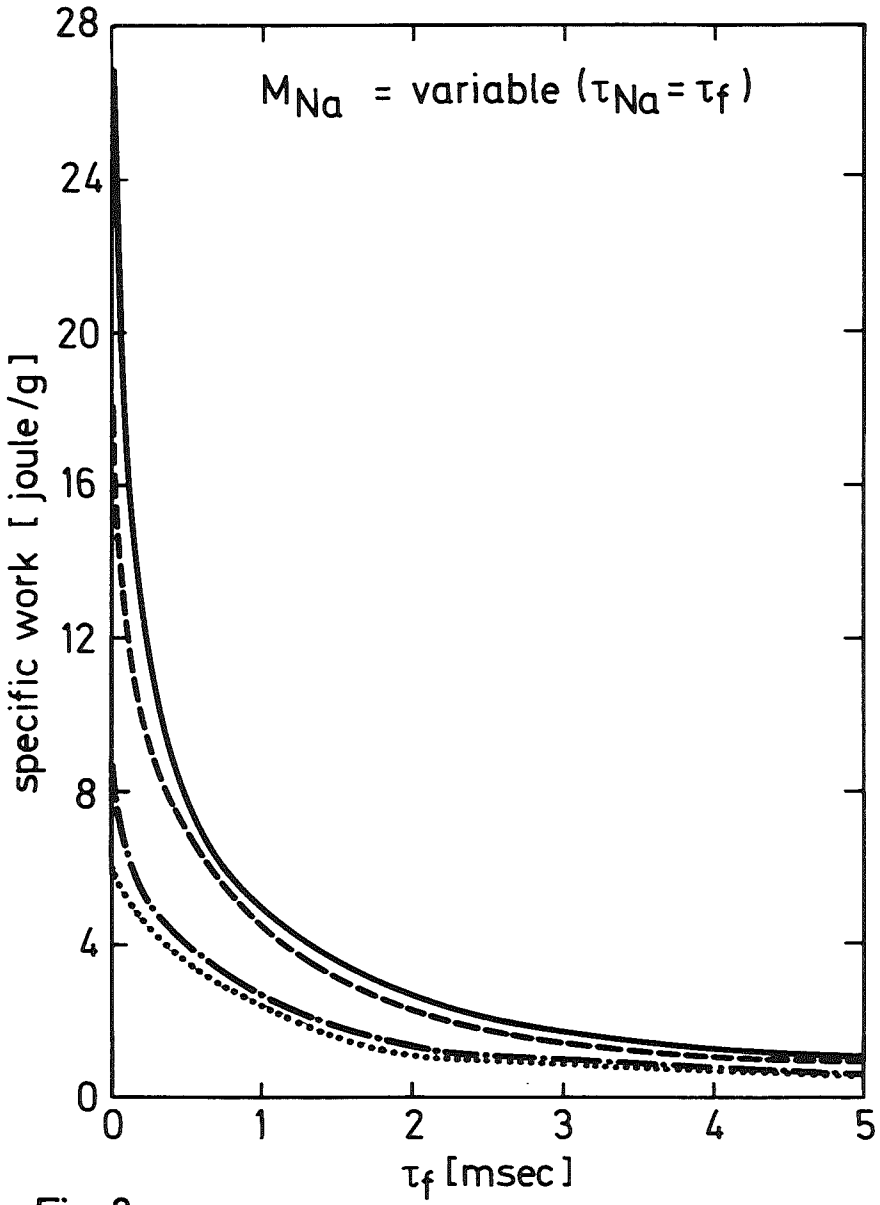

Fig. 8

Cho and Wright Case - M_f Linear Function of Time
Phase A - Specific Work as a Function of Fuel Mixing Time Constant

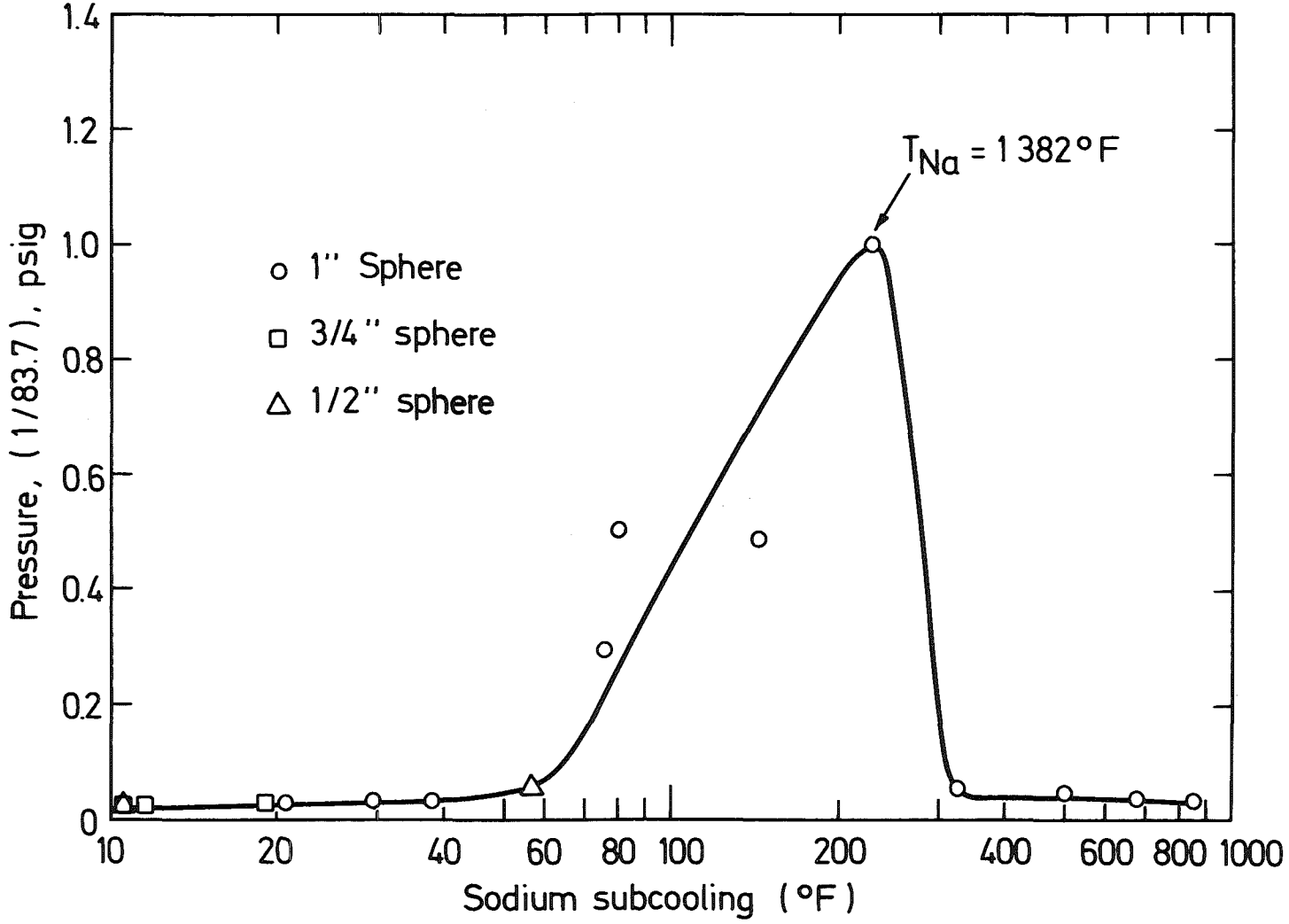

Fig.9 Effect of the Degree of Subcooling on the Violent Interaction in the Transition Region (from Ref. 39)

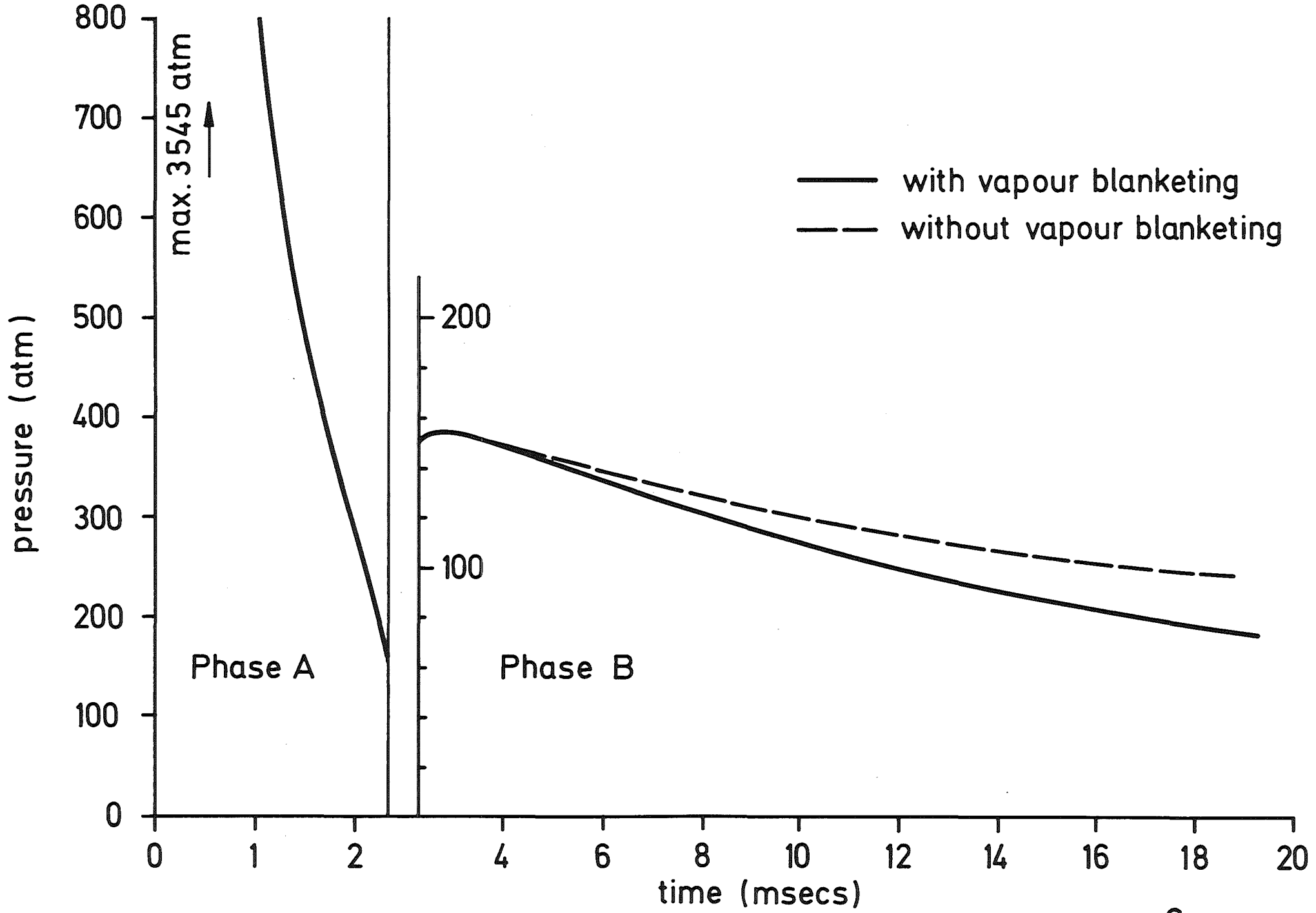

Fig. 10 FCI with a very low mixing time constant (10^{-6} secs)
(From Ref 43)

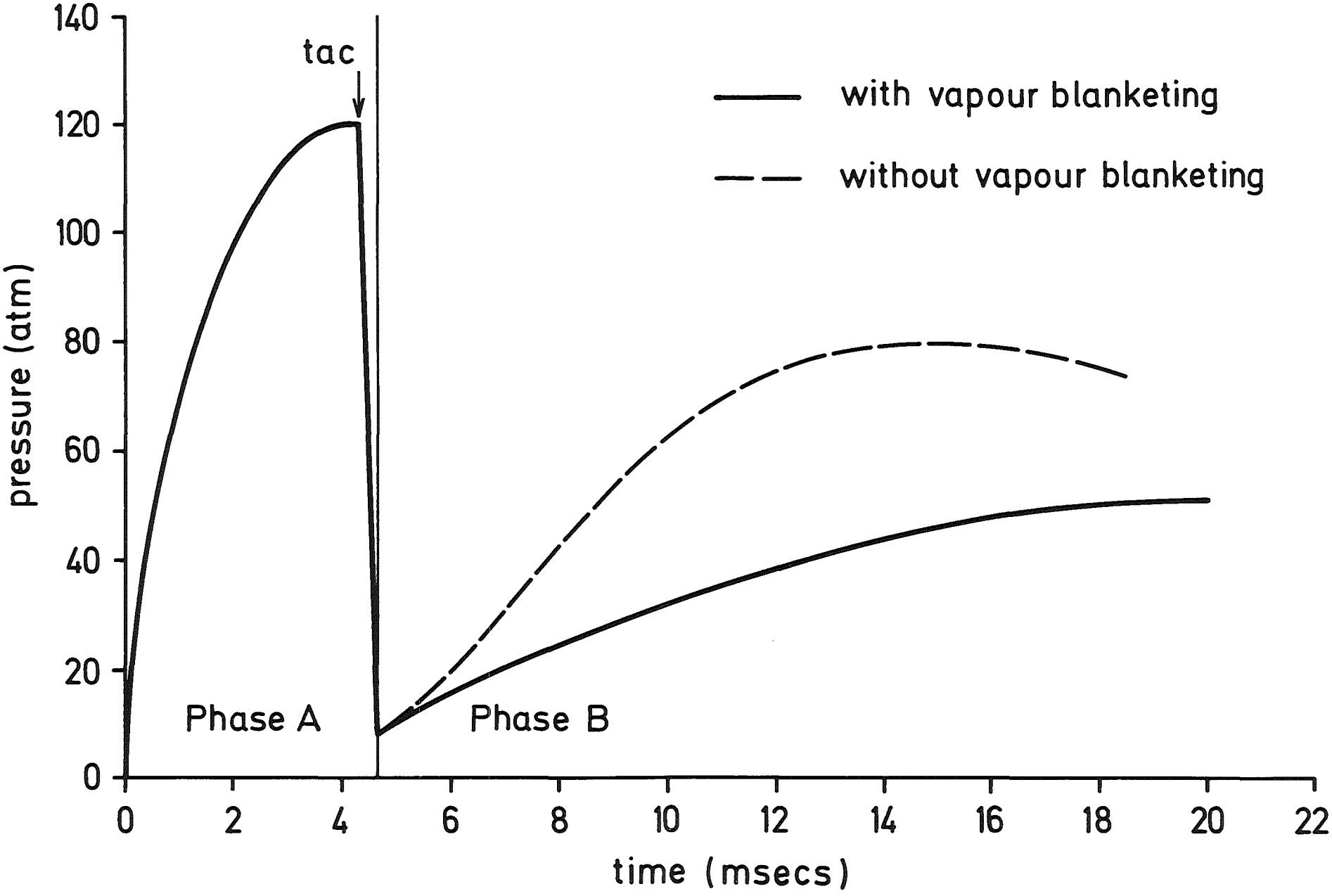

Fig. 11 FCI with a large mixing time constant (10 msecs)
(From Ref. 43)